Cryptostatin, a chagasin-family cysteine protease inhibitor of *Cryptosporidium parvum*

J.-M. KANG[1], H.-L. JU[1], J.-R. YU[2], W.-M. SOHN[1] *and* B.-K. NA[1]*

[1] *Department of Parasitology and Institute of Health Sciences, Gyeongsang National University School of Medicine, Jinju 660–751, Korea*
[2] *Department of Environmental and Tropical Medicine, Konkuk University School of Medicine, Seoul 143–701, Korea*

(*Received 30 September 2011; revised 11 December 2011 and 18 January 2012; accepted 28 January 2012; first published online 23 March 2012*)

SUMMARY

Cysteine proteases of pathogenic protozoan parasites play pivotal roles in the life cycle of parasites, but strict regulation of their activities is also essential for maintenance of parasite physiology and interaction with hosts. In this study, we identified and characterized cryptostatin, a novel inhibitor of cysteine protease (ICP) of *Cryptosporidium parvum*. Cryptostatin showed low sequence identity to other chagasin-family ICPs, but 3 motifs (NPTTG, GXGG, and RPW/F motifs), which are evolutionarily conserved in chagasin-family ICPs, were found in the sequence. The overall structure of cryptostatin consisted of 8 β-strands that progressed in parallel and closely resembled the immunoglobulin fold. Recombinant cryptostatin inhibited various cysteine proteases, including papain, human cathepsin B, human cathepsin L, and cryptopain-1, with K_i's in the picomolar range. Cryptostatin was active over a wide pH range and was highly stable under physiological conditions. The protein was thermostable and retained its inhibitory activity even after incubation at 95 °C. Cryptostatin formed tight complexes with cysteine proteases, so the complexes remained intact in the presence of sodium dodecyl sulfate and β-mercaptoethanol, but they were disassembled by boiling. An immunogold electron microscopy analysis demonstrated diffused localization of cryptostatin within oocystes and meronts, but not within trophozoites, which suggests a possible role for cryptostatin in host cell invasion by *C. parvum*.

Key words: *Cryptosporidium parvum*, inhibitor of cysteine protease, cryptostatin, chagasin-family, cryptopain-1.

INTRODUCTION

Proteases play essential roles in diverse biological processes in all organisms, but strict regulation of their activities is also essential. Protease activity can be regulated at several levels, extending from regulation of gene expression to synthesis of specific inhibitors. Endogenous protein inhibitors of proteolytic enzymes play pivotal roles in the delicate regulation of normal physiological processes in organisms by regulating the activities of endogenous proteases and by protecting the organisms from the deleterious effects of exogenous proteases (Laskowski and Kato, 1980; Knox, 2007; Kang *et al*. 2010).

Inhibitors of cysteine proteases (ICPs) of the chagasin-like family (MEROPS family I42) are recently identified small proteins with low molecular masses of 11–15 kDa. They are uniquely identified in some parasitic protozoa, bacteria, and archaea (Monteiro *et al*. 2001; Rigden *et al*. 2002). Interestingly, ICPs show low sequence identities with each other and no significant sequence similarity with cystatins, thyropins, or any other previously identified cysteine protease inhibitors (Rigden *et al*. 2002). Chagasin, the first ICP identified in *Trypanosoma cruzi*, binds tightly to cruzipain, the major papain-like cysteine protease of *T. cruzi*, and regulates endogenous activity of cruzipain, which is essential for parasite differentiation and invasion into mammalian host cells (Monteiro *et al*. 2001; Santos *et al*. 2005, 2006). The orthologues of chagasin were subsequently characterized in several protozoan parasites, including *T. brucei, Leishmania mexicana, Entamoeba histolytica, Plasmodium falciparum*, and *Toxoplasma gondii* (Sanderson *et al*. 2003; Besteiro *et al*. 2004; Riekenberg *et al*. 2005; Pandey *et al*. 2006; Saric *et al*. 2006; Sato *et al*. 2006; Huang *et al*. 2009). Although the biological functions of these proteins are not fully understood, they effectively inhibit their own endogenous cysteine proteases as well as papain and mammalian cathepsin B and cathepsin L, which suggests their possible roles in the host–parasite interaction.

Cryptosporidium parvum is an apicomplexa protozoan parasite that causes diarrhoeal illness in a number of mammals including humans (Tzipori and Ward, 2002). Infections in healthy individuals are usually asymptomatic or characterized by self-limiting diarrhoea, but it can develop into severe and life-threatening disease in immunocompromised patients (Peterson, 1992; Fayer *et al*. 2000; Kosek *et al*. 2001). Due to the essential roles of cysteine

* Corresponding author: Department of Parasitology and Institute of Health Sciences, Gyeongsang National University School of Medicine, Jinju 660–751, Korea. Tel: +82 55 772 8102. Fax: +82 55 772 8109. E-mail address: bkna@gnu.ac.kr

doi:10.1017/S0031182012000297

proteases in growth, differentiation, and survival of pathogenic protozoan parasites, highly extensive studies on the structures and functions related to papain-like enzymes and their regulation have been conducted in various pathogenic protozoan parasites, but little is known about the cysteine proteases and their regulation in *C. parvum*. Previously, we identified and characterized cryptopain-1, a papain-like cysteine protease of *C. parvum* (Na *et al*. 2009). Cryptopain-1 shares similar structural and biochemical properties with orthologous enzymes of other protozoan parasites. The biological function of cryptopain-1 is yet to be elucidated, but expression of the enzyme in sporozoites suggests its possible role in host cell invasion of *C. parvum*.

Here, we report the characterization of cryptostatin, a novel endogenous ICP of *C. parvum*. Cryptostatin showed low sequence identities with orthologues of chagasin-family ICPs, but it had characteristic motifs that are well conserved in chagasin-family ICPs. This protein effectively inhibited cryptopain-1 as well as papain, human cathepsin B, and human cathepsin L. Cryptostatin was localized in oocysts and meronts of *C. parvum*, but not in trophozoites, which suggested its possible function in host cell invasion by the parasite.

MATERIALS AND METHODS

Cloning and identification of a gene encoding cryptostatin

A gene putatively encoding a cryptostatin (Gene ID: cgd6_1910) was identified by data mining the *Cryptosporidium* genome resource (CryptoDB, http://cryptodb.org).

The cryptostatin gene was amplified by polymerase chain reaction (PCR) from *C. parvum* Iowa II genomic DNA using forward (5′-ATGAATAA GACAATTTTTAGACTTTTA-3′) and reverse (5′-CTATTCCTTTATTATTTCTTCGCAGGG-3′) primers spanning the predicted open reading frame. The amplification reaction was performed using the following thermal cycling profile: 94 °C for 5 min, 30 cycles at 94 °C for 1 min, 50 °C for 1 min, and 72 °C for 1 min, followed by a 72 °C extension for 10 min. The PCR product was purified, ligated into T&A cloning vector (Real Biotech Cooperation, Banqiaa City, Taiwan), and then transformed into *Escherichia coli* DH5*α*. The sequence of the cloned gene was confirmed by DNA sequencing. Analysis of the primary and secondary structures of the deduced amino acid sequence was conducted with DNASTAR (DNASTAR, Madison, WI, USA) and Signal P (http://www.cbs.dtu.dk/services/SignalP). Three-dimensional homology modelling of cryptostatin was performed using the Modeller (http://salilab.org/modeller/) based on the crystal structure of *Entamoeba histolytica* ICP2 (EhICP2, pdb: 3M86). Subsequent analysis, visualization, and preparation of the model were performed using UCSF Chimera (http://www.cgl.ucsf.edu/chimera/). The nucleotide sequence of cryptostatin was deposited in GenBank under Accession number GU433606.

Expression and purification of recombinant cryptostatin

The cryptostatin coding sequence with a deleted N-terminal signal peptide region was amplified with primers incorporating *Sal* I and *Hind* III restriction sites (5′-GTCGACTCTGATATGACATCTAG TGGTAGC-3′ and 5′-AAGCTTCTATTCCTT TATTATTTCTTCGCA-3′). The PCR product was subcloned into T&A cloning vector (Real Biotech Cooperation), and then transformed into *E. coli* DH5*α*. Positive clones were selected and the plasmid was purified. The plasmid was digested with *Sal* I and *Hind* III and ligated into an appropriately digested pQE-30 expression vector (Qiagen, Valencia, CA, USA), which was then transformed into *E. coli* M15 [pREP4] cells (Qiagen). Selected clones were grown and induced with 1 mM isopropyl-1-thio-*β*-D-galactopyranoside (IPTG) for 3 h at 37 °C. The cells were harvested by centrifugation, suspended in native lysis buffer (50 mM NaH_2PO_4, 300 mM NaCl, 10 mM imidazole, pH 8·0), sonicated (10 cycles of 5 s each, with cooling for 30 s between the cycles) on ice, and then centrifuged at 4 °C for 20 min at 12 000 ***g***. The recombinant cryptostatin was purified by nickel-nitrilotriacetic acid (Ni-NTA) affinity chromatography (Qiagen) by following the manufacturer's instructions. The purification and purity of the recombinant protein were analysed by 15% sodium dodecyl sulfate-polyacrylamide gel electrophoresis (SDS-PAGE). The sequence of the expression construct was confirmed by automated DNA sequencing.

Production of antibody for cryptostatin (anti-cryptostatin)

To produce specific antibodies directed towards cryptostatin, balb/c mice were immunized with purified recombinant cryptostatin (50 *μ*g) 3 times every 2 weeks. The protein was emulsified with equal volumes of Freund's complete adjuvant (Sigma, St Louis, MO, USA) for the first immunization or Freund's incomplete adjuvant (Sigma) for the following 2 booster immunizations. Two weeks after the final boosting, the mice were sacrificed and the sera were collected. The immunoglobulin G (IgG) fraction was further isolated from the sera with a Protein G-Sepharose column (Amersham Biosciences, Piscataway, NJ, USA). The specificity of the antibody was confirmed by immunoblotting.

https://doi.org/10.1017/S0031182012000297 Published online by Cambridge University Press

Inhibitory activity assay

The inhibitory potential of cryptostatin on several cysteine proteases, human cathepsin B (from human liver, Sigma), human cathepsin L (from human liver, Sigma), papain (Sigma), and cryptopain-1 was analysed by measuring residual enzyme activity after incubation of each enzyme with cryptostatin as described previously (Kang *et al*. 2011*a*). Cryptopain-1 was prepared as described previously (Na *et al*. 2009). In brief, each enzyme (20 nM) was incubated with different concentrations (0–100 nM) of cryptostatin or bovine serum albumin (BSA, negative control) in 50 mM phosphate-buffered saline (PBS, pH 7·2). After 20 min of incubation at room temperature, the substrate solution was added to the mixture, after which the residual enzyme activity was determined by measuring the release of fluorescence (excitation at 355 nm, emission at 460 nm) over 30 min at room temperature with a Fluoroskan Ascent FL (Thermo, Vantaa, Finland). The substrate (final concentration: 5 μM) and assay buffer for each enzyme were as follows. Human cathepsin B: benzyloxycarbonyl-$_{L}$-arginyl-$_{L}$-arginine 4-methyl-coumaryl-7-amide (Z-RR-MCA), 50 mM sodium acetate (pH 6·0); human cathepsin L: Z-$_{L}$-phenylalaninyl-$_{L}$-arginine-MCA (Z-FR-MCA), 50 mM sodium acetate (pH 5·5); papain: Z-FR-MCA, 50 mM sodium acetate (pH 6·0); cryptopain-1: Z-$_{L}$-leucyl-$_{L}$-arginine-MCA (Z-LR-MCA), 50 mM sodium acetate (pH 6·5). All assay buffers contained 10 mM dithiothreitol (DTT), and all substrates were purchased from Peptide International (Louisville, KY, USA). In all experiments, *trans*-epoxy-succinyl-$_{L}$-leucylamido(4-guanidino)butane (E-64; Sigma) was used as a control inhibitor. The concentration of cryptostatin was determined by titration with papain as described previously (Monteiro *et al*. 2001). The concentration of cysteine proteases used in this study was determined by active site titration with E-64 (Barrett *et al*. 1982). The equilibrium dissociation constant (K_i) values were calculated by the equation $K_i = IC50(1/(1+[S]/K_m)$ as described previously (Sanderson *et al*. 2003). The K_m of each enzyme for the substrate was determined under the same assay conditions in the absence of cryptostatin. The resulting data were analysed by non-linear regression using GraphPad Prism 5·0 Software (San Diego, CA, USA).

pH dependency and stability of cryptostatin

The effect of pH on the inhibitory activity of cryptostatin was determined. The purified cryptostatin (20 nM) was incubated with the same concentration of human cathepsin B, human cathepsin L, papain, or cryptopain-1 in different pH buffers [50 mM sodium acetate (pH 4·0–5·0), 50 mM sodium phosphate (pH 6·0–7·0), or Tris–HCl (pH 8·0)] for 20 min at 37 °C. For each pH step, control enzyme without cryptostatin was also incubated to account for the effect of pH. After incubation, the residual enzyme activity of each sample was measured as described above and the percentage inhibition was determined by comparison with the non-inhibition enzyme control. Thermal stability of cryptostatin was analysed by incubation of cryptostatin at different temperatures (37 and 95 °C) for 1–3 h in 50 mM sodium phosphate buffer (pH 7·0). The samples were cooled on ice for 30 min and the residual inhibitory activities of aliquots of sample against each enzyme were measured as described above. The pH stability of cryptostatin was also examined by incubating cryptostatin in different pH buffers [50 mM sodium acetate (pH 4·0–5·0), 50 mM sodium phosphate (pH 6·0–7·0), Tris–HCl (pH 8·0), or Glycine–NaOH (pH 9·0)] at 37 °C for 3 h, followed by measuring the residual inhibitory activity of cryptostatin against each enzyme by the same method described above.

Analysis of the cryptostatin-cysteine protease complex

Analysis of the cryptostatin-cysteine protease complex was performed as described previously (Santos *et al*. 2005). Cryptostatin was incubated with cryptopain-1 or papain in approximately equal molar ratios in phosphate-buffered saline (PBS, pH 7·2) for 20 min at room temperature. The molecular complexes were then subjected to the following treatments: buffer 1 [62·5 mM Tris-HCl, pH 6·8, 10% glycerol]; buffer 2 [buffer 1 supplemented with 2% SDS]; buffer 3 [buffer 1 supplemented with 2% SDS and 5% β-mercaptoethanol (β-ME)]. The samples were treated with or without boiling, subjected to 15% SDS-PAGE, and then transferred to nitrocellulose membranes (Millipore, Billerica, MA, USA) to detect the cryptostatin-cysteine protease complexes that formed. The membranes were blocked with PBS supplemented with 0·05% Tween 20 (PBST, pH 7·2) and 3% skim milk for 1 h at room temperature. The membranes were then incubated with anti-cryptostatin or anti-cryptopain-1 diluted 1:1000 in PBST at room temperature for 2 h. After several washes with PBST, the membranes were incubated with 1:1000 diluted horseradish peroxidase-conjugated anti-mouse IgG (Sigma). The membranes were washed with PBST several times, and the reactive bands were visualized with 4-chloro-1-naphthol (Sigma). Cryptostatin alone was also treated by the same procedure and analysed by immunoblot using anti-cryptostatin antibody.

Localization of cryptostatin

To determine the localization of cryptostatin, we conducted an immunogold electron microscopy analysis. The small intestines of *C. parvum*-infected

https://doi.org/10.1017/S0031182012000297 Published online by Cambridge University Press

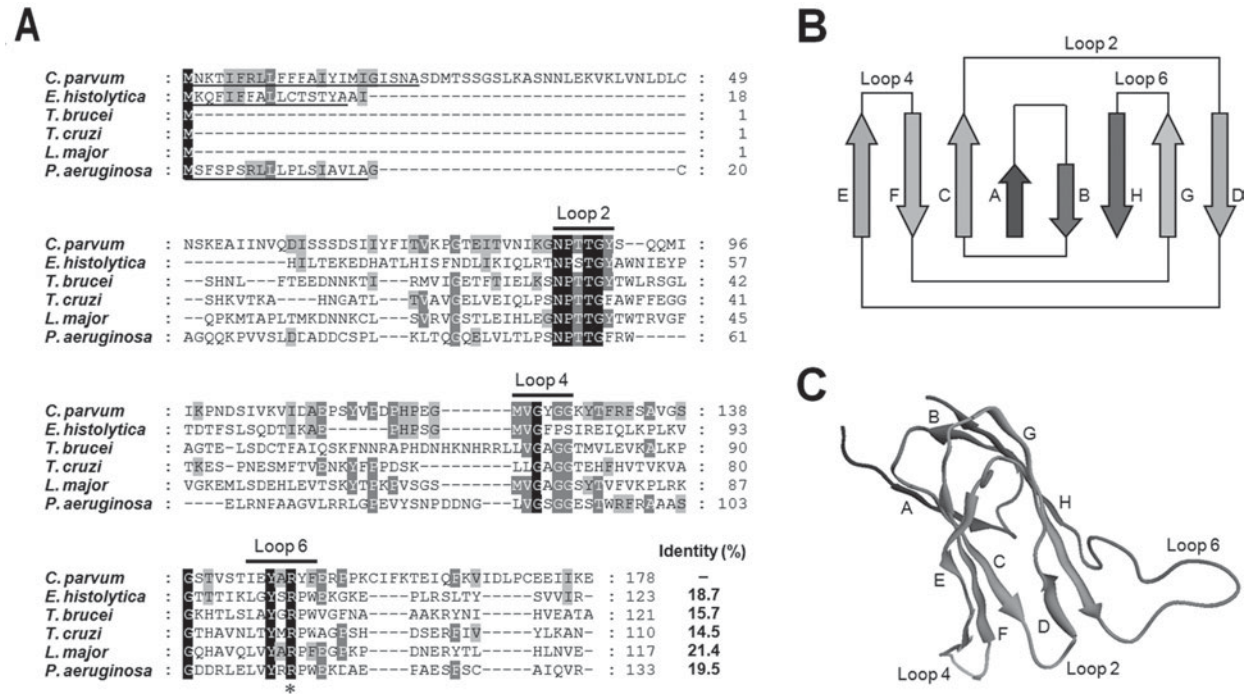

Fig. 1. Sequence and structural analyses of cryptostatin. (A) Multiple sequence alignment. The amino acid sequence of cryptostatin was aligned with other chagasin-family ICPs. Three motifs (NPTTG, GXGG, and RPW/F motifs), which are conserved in chagasin-family ICPs and are involved in formation of loops 2, 4, and 6, are overlined. The conserved Arg at loop 6 is marked as an asterisk. The predicted signal peptide region is shown by underlines. The shading represents the degree of identity among the sequences: black (100%), dark grey (50–92%) and light grey (15–49%). Gaps are introduced into the sequences to maximize alignment. Sequence identity of cryptostatin to other chagasin-family ICPs was represented. (B) Topology diagram of cryptostatin. This diagram represents cryptostatin as a pseudosymmetrical molecule in which 4 β-strands contribute to the formation of each β-sheet (Casados-Vázquez *et al*. 2011). This novel topology arrangement closely resembles the arrangement in the immunoglobulin fold. (C) Homology modelling. Homology modelling of cryptostatin was performed based on crystal structure of *E. histolytica* EhICP2 (pdb: 3M86). Conserved motifs form loops 2, 4, and 6 that are exposed to the outside of the molecule and jointly contact the target protease.

female C57BL6/J mice were dissected after 5 days of infection and fixed in 2% paraformaldehyde and 0·4% glutaraldehyde for 2 h at room temperature. Fixed tissues were washed with 100 mM sodium phosphate (pH 7·2) and dehydrated through a 30–95% graded ethanol series. Dehydrated tissues were embedded in LR gold resin (London Resin, London, UK) and polymerized at −20 °C for 24 h under UV illumination. Ultra-thin sections were prepared at a thickness of 90 nm, and sections were mounted on nickel grids. The immunogold labelling procedure was performed as described previously (Lee *et al*. 2009). Tissue sections were incubated in PBS-milk-Tween 20 (PMT; 3% skim milk and 0·01% Tween 20 in PBS, pH 7·2) for 10 min and exposed to anti-cryptostatin or anti-cryptopain-1 diluted in PMT for 2 h at room temperature. The sections were washed thoroughly with PBS-BSA-Tween 20 (1% BSA, 0·01% Tween 20 in PBS, pH 7·2) and incubated overnight with 5 nm gold-conjugated goat anti-mouse IgG (Sigma) at 4 °C. Silver enhancement was performed with a commercial kit (Amersham Biosciences, Uppsala, Sweden) followed by staining with uranyl acetate and lead citrate. The stained sections were examined under a transmission electron microscope (Hitachi H-7650, Tokyo, Japan).

RESULTS

Sequence analysis of cryptostatin

The open reading frame of the cryptostatin gene consisted of 537 bp that encoded 178 amino acid residues with a predicted molecular mass of 19·8 kDa and a pI of 5·97. A sequence comparison algorithm (Signal P) predicted that cryptostatin had a typical N-terminal signal peptide sequence and contained a much longer N-terminal portion than of chagasin. Three characteristic motifs, which are conserved in the chagasin-family ICPs (NPTTG, GXGG, and RPW/F motifs) and are essential for the formation of chagasin's binding-sites (loops 2, 4, and 6, respectively) to target enzymes (Salmon *et al*. 2006), were found in cryptostatin. Besides these motifs, cryptostatin differed quite considerably from other chagasin-family ICPs. The overall sequence similarity of cryptostatin to other chagasin-family ICPs was 14·5–21·4% (Fig. 1A). Similar to chagasin and

https://doi.org/10.1017/S0031182012000297 Published online by Cambridge University Press

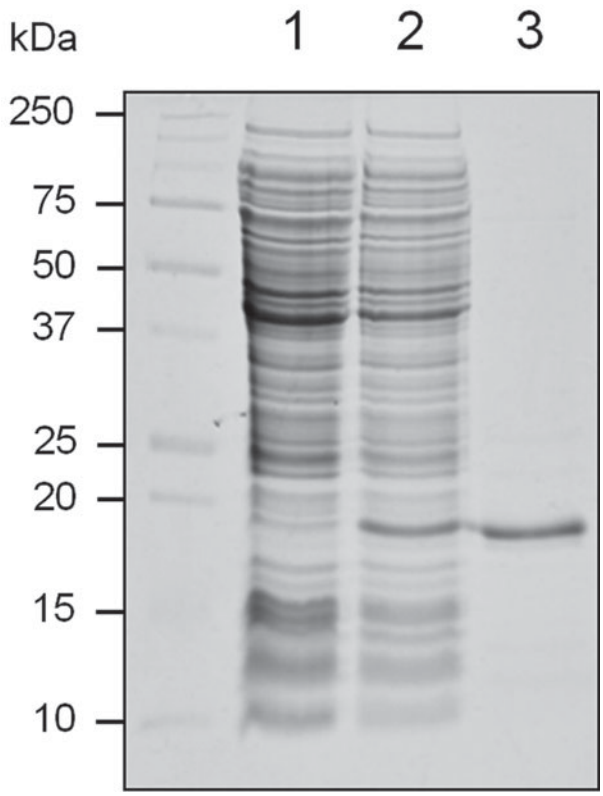

Fig. 2. Expression and purification of recombinant cryptostatin. A portion of gene encoding cryptostatin with a deleted N-terminal signal peptide region was cloned into pQE-30 vector and transformed into *E. coli* M15 [pREP4] cells. Overexpression of recombinant cryptostatin was induced with 1 mM IPTG and the recombinant protein was purified with Ni-NTA chromatography. Proteins were analysed by 15% SDS-PAGE and stained with Coomassie blue. Lane 1, *E. coli* lysate control; lane 2, IPTG-induced *E. coli* lysate; lane 3, purified recombinant cryptostatin (10 μg).

Table 1. K_i values of cryptostatin against cysteine proteases

(The K_i values are represented as mean ± standard deviation derived from 3 independent assays. The enzymes were assayed for inhibition as described in the Materials and Methods section.)

Enzyme	K_i (nM)
Cryptopain-1	0·025 ± 0·004
Papain	0·048 ± 0·009
Cathepsin B	0·173 ± 0·021
Cathepsin L	0·031 ± 0·003

chagasin-like family ICPs, the secondary structure of cryptostatin was predicted to lack α-helices and to consist mainly of β-strands (Fig. 1B). Homology modelling also showed that cryptostatin had an immunoglobulin-fold in which 8 β-strands (A–H) that were progressed in parallel, and the loops (loops 2, 4, and 6), which connected within the β-sheet arrangement, were exposed to the outside (Fig. 1C).

Inhibitory activity of cryptostatin

Recombinant cryptostatin was expressed in *E. coli* as a soluble protein with an apparent molecular mass of 18 kDa (Fig. 2), which was similar to the theoretical value estimated from its predicted amino acid sequence. The recombinant protein was purified by Ni-NTA affinity chromatography. To investigate the inhibitory potency of cryptostatin, we analysed its ability to inhibit a series of cysteine proteases, human cathepsin B and cathepsin L, papain, and cryptopain-1. Cryptostatin effectively inhibited the enzymatic activities of all tested enzymes with K_i's in the picomolar range (Table 1). Meanwhile, BSA did not show any inhibitory effect (data not shown). We also tested the effect of pH on the inhibitory function of cryptostatin. At all tested pHs, cryptostatin was active and its inhibitory activity was not significantly influenced by pH, which suggests that cryptostatin effectively inhibited those enzymes over a broad range of pHs (data not shown). Cryptostatin was highly stable at 37 °C and maintained its inhibitory activity up to 95% when treated at 95 °C for 3 h (data not shown). Pre-incubation of cryptostatin at pH 4·0–9·0 also had no significant effect on its inhibitory activity (data not shown).

Molecular complexes of cryptostatin and cysteine proteases

To understand the molecular interactions between cryptostatin and cysteine proteases, cryptostatin was incubated with cryptopain-1 or papain at an equal molar ratio and the resulting molecular complexes were analysed by immunoblot. Cryptostatin showed a shift in molecular mass of approximately 2·5 kDa in the absence of SDS and β-ME due to the presence of disulphide bonds (Fig. 3A). Under non-reducing conditions, partial reductions in molecular masses of proteins are routinely observed when the proteins contain disulphide bonds (Hames, 1990). High molecular weight complexes between cryptostatin and cryptopain-1 were identified, and the complexes were preserved, even though the samples were treated with 2% SDS or 2% SDS and 5% β-ME (Fig. 3B). However, the complexes completely dissociated upon boiling (Fig. 3B). Cryptostatin also formed molecular complexes with papain, showing an identical pattern to that of cryptopain-1 (data not shown). These data collectively suggest that cryptostatin formed tight complexes with cysteine proteases and that the complexes remained stable in the presence of SDS and β-ME, but were disassembled by heating.

Localization of cryptostatin

To determine the localization of cryptostatin in *C. parvum*, we performed an immunogold-labelling assay using anti-cryptostatin. Gold particles were

https://doi.org/10.1017/S0031182012000297 Published online by Cambridge University Press

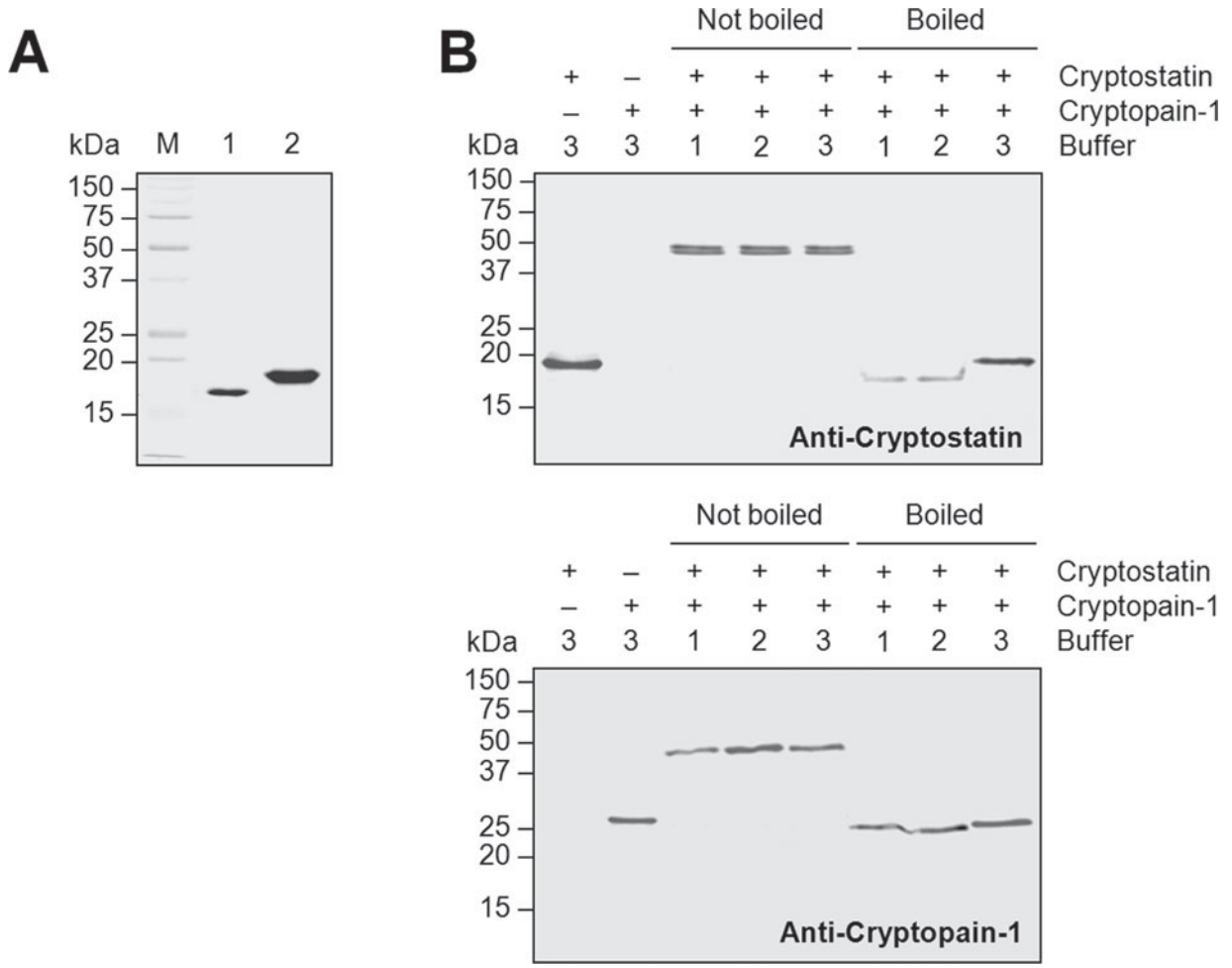

Fig. 3. Analysis of molecular complexes of cryptostatin and cryptopain-1. (A) Recombinant cryptostatin (10 μg) was mixed with sample buffer without (lane 1) or with (lane 2) SDS and β-ME, and resolved by 15% SDS-PAGE without boiling. Lane M, molecular marker proteins. (B) Recombinant cryptostatin (5 μg) was incubated with an equal molar ratio of cryptopain-1 in PBS (pH 7·2) for 20 min and subsequently diluted in buffer 1 (62·5 mM Tris-HCl, pH 6·8, 10% glycerol), buffer 2 (buffer 1 containing 2% SDS), or buffer 3 (buffer 1 containing 2% SDS and 5% β-ME). The boiled or not boiled samples were separated by 15% SDS-PAGE, transferred to nitrocellulose membranes, and then probed with anti-cryptostatin or anti-cryptopain-1 antibody.

identified within oocysts and meronts, but they were dispersed within the parasites without clear localization to intracellular organelles or membranes (Fig. 4). Gold labelling was also found in trophozoites, but the amount was much lower than that of other developmental stages (Fig. 4). We also conducted the immunogold-labelling assay using anti-cryptopain-1 to analyse the relationship between cryptostatin and cryptopain-1. Cryptopain-1 was also mainly found within oocysts and meronts, but not apparent within trophozoites (Fig. 4). The control applied with the same concentrations of pre-immune mouse serum showed that a second antibody did not stain (data not shown).

DISCUSSION

Here, we identified and characterized cryptostatin, a chagasin family ICP of *C. parvum*. A comparison of the cryptostatin sequence with those of presently identified ICPs from other organisms revealed that cryptostatin had low sequence identities with other ICPs, but that the protein had 3 typical motifs (NPTTG at positions 86–90, GXGG at positions 124–127, and RPW/F at positions 149–151), which are evolutionally conserved in chagasin family ICPs. While all 3 motifs were well conserved in cryptostatin, the orthologues of apicomplexan protozoa parasites *Toxoplasma gondii* (toxostatin-1 and -2) and *Plasmodium falciparum* (falstatin) do not have the typical NPTTG motif (Pandey *et al*. 2006; Huang *et al*. 2009). Instead, toxostatins and falstatin contain the GXGYXW(F/L) element at the position of the motif. Toxostatins also lack the GXGG motif but contain the third motif similar to chicken cystatin and rat kininogen (Huang *et al*. 2009). Cryptostatin showed a low level of sequence identities with toxostatin-1 (11·9%), toxostatin-2 (12·4%), and falstatin (14·6%). Moreover, compared to cryptostatin and toxostatins that have lower molecular masses

https://doi.org/10.1017/S0031182012000297 Published online by Cambridge University Press

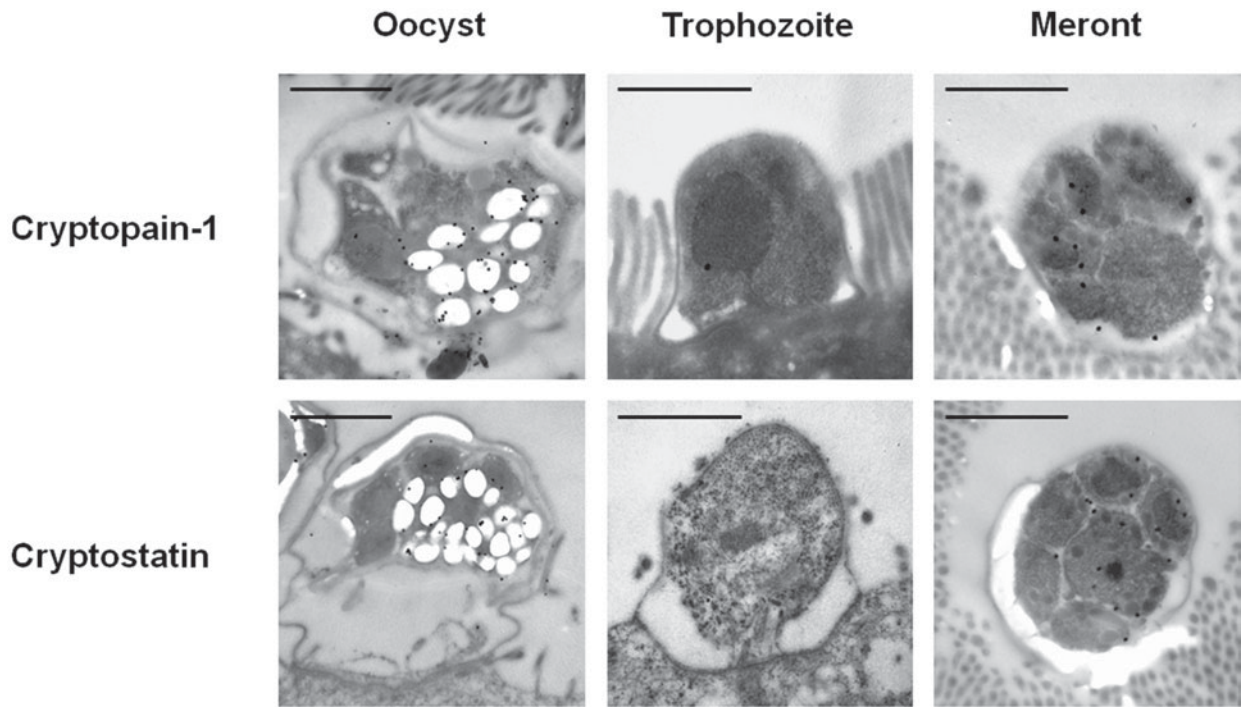

Fig. 4. Localization of cryptostatin. Immunogold electron microscopy analysis was performed by using anti-cryptostatin or anti-cryptopain-1. Reactive gold particles with diffused pattern were mainly identified within oocysts and meronts, but were not apparent within trophozoites. Scale bars = 1 μm.

(19·2–28 kDa), the molecular mass of falstatin is 47 kDa. Although toxostatins and falstatin also effectively inhibited the parasite's own cysteine proteases as well as several human cysteine proteases, the evolutionary significance of these dissimilarities identified in chagasin family proteins of apicomplexan protozoa parasites must be investigated further. The NPTTG and 2 other motifs of chagasin are essential to form loops 2, 4, and 6, respectively, which are critical for the interactions with the catalytic cysteine of the target proteases (Smith *et al*. 2006; Wang *et al*. 2007; dos Reis *et al*. 2008). Crystal and nuclear magnetic resonance spectroscopy structures of ICPs from *T. cruzi*, *L. mexicana*, and *E. histolytica* suggest that ICPs adopt an immunoglobulin-like fold mainly composed of β-strands and 3 exposed loops (loops 2, 4, and 6), which are directly involved in precise interactions with their target cysteine protease (Smith *et al*. 2006; Ljunggren *et al*. 2007; Figueiredo da Silva *et al*. 2007; Wang *et al*. 2007; Redzynia *et al*. 2008, 2009; Casados-Vázquez *et al*. 2011). The prediction of the secondary and tertiary structures of cryptostatin also demonstrated that cryptostatin consisted of 8 β-strands that progressed in parallel and had an immunoglobulin-fold. These results collectively suggest that cryptostatin is a typical ICP of *C. parvum*, which belongs to the chagasin-family proteins.

Recombinant cryptostatin showed similar biochemical properties with presently characterized ICPs. Cryptostatin showed broad-spectrum inhibitory activity against the parasite's own cysteine protease, cryptopain-1, as well as papain, human cathepsin B, and human cathepsin L. The molar ratio of inhibition approximated to a 1:1 relationship and the inhibition was competitive. Although a high-affinity interaction against human cathepsin B was identified, the K_i against cathepsin B was slightly higher than that of other enzymes tested. This can be explained by the presence of the occluding loop in cathepsin B, which may obstruct the active site and must dissociate before cystatin family inhibitors can bind and inhibit the enzyme (Björk *et al*. 1994). Chagasin family ICPs are highly thermostable, retaining their inhibitory activities even after boiling (Monteiro *et al*. 2001; Santos *et al*. 2005). Our results also suggest that cryptostatin is a highly stable protein under a wide range of pHs and high temperatures. We also found that cryptostatin formed tight complexes with cryptopain-1 and papain, so that the complexes were not easily disrupted by SDS and β-ME, but were disassembled by heating. This observation is similar to chagasin, which forms extremely stable complexes with cruzipain (Santos *et al*. 2005).

Our immunogold electron microscopy analysis revealed that cryptostatin was mainly found in oocysts and meronts, but was not apparent in trophozoites. Interestingly, cryptopain-1 has also been identified with the same pattern. Previously, we identified and characterized cryptopain-1 (Na *et al*. 2009). Despite that its biological function is obscure, cryptopain-1 is functionally expressed in *C. parvum* sporozoites, suggesting its possible role in host cell invasion (Na *et al*. 2009). In this study, we

https://doi.org/10.1017/S0031182012000297 Published online by Cambridge University Press

confirmed cryptopain-1 expression in oocysts and meronts stages, but not much in trophozites, which supports the notion that cryptopain-1 may be involved in the host cell invasion process rather than having a catabolic function, which is essentially needed for the trophozoite stage. We did not obtain strong evidence that cryptopain-1 is an endogenous target enzyme of cryptostatin, as we could not determine co-localization of both proteins in subcellular compartments of the parasite. However, the presence of both proteins at the same developmental stages suggested possible functions of cryptostatin. As in other papain-family cysteine proteases, the enzymatically active cryptopain-1 is produced by proteolytic removal of the N-terminal pro-domain from the zymogen precursor, pro-cryptopain-1 (Na *et al*. 2009). Considering that zymogen activation occurs by an autocatalytic process, cryptostatin may help to regulate the degree of zymogen conversion, representing a checkpoint at a limiting step of cryptopain-1 production. Effective inhibitory activity of cryptostatin against human cathepsin B and cathepsin L also lead us to hypothesize that cryptostatin has an additional potential role in the host–parasite interaction by modulating the activity of host cysteine proteases, either after endocytosis of the enzymes or in the parasite's environment. Indeed, several experimental studies have provided direct evidence of possible host–parasite interactions of chagasin and leishmania ICPs (Santos *et al*. 2005; Besteiro *et al*. 2004).

Further knowledge of the biological roles of cryptostatin and cryptopain-1 and their distributions in specific subcellular compartments will help to elucidate the contribution of cryptostatin in the regulation of cryptopain-1 or host enzymes. CryptoDB indicates that *C. parvum* has a number of different proteases and protease inhibitor classes. However, the technical shortcomings of *in vitro* culture of the parasite have been the major obstacle for comprehensive study of the proteins; thus only a small number of proteases have currently been characterized (Na *et al*. 2009; Wanyiri *et al*. 2009; Kang *et al*. 2011*b*). Considering that proteases of protozoan parasites have been identified as attractive drug targets (Cazzulo, 2002; Rosenthal, 2004; Ersmark *et al*. 2006; Chen *et al*. 2009; Dou and Carruthers, 2011; Teixeira *et al*. 2011), comprehensive studies to elucidate the biochemical properties and biological functions of proteases and protease inhibitors, which probably play key roles in the life cycle of *C. parvum*, are warranted for the understanding of the parasite's physiology and development of anti-cryptosporidial drugs.

ACKNOWLEDGEMENTS

This study was supported by a grant of the Korea Healthcare Technology R&D Project, Ministry for Health, Welfare & Family Affairs, Republic of Korea (A100119).

REFERENCES

Barrett, A. J., Kembhavi, A. A., Brown, M. A., Kirschke, H., Knight, C. G., Tamai, M. and Hanada, K. (1982). l-trans-epoxysuccinyl-leucylamido(4-guanidino)butane (E-64) and its analogues as inhibitors of cysteine proteinases including cathepsins B, H, and L. *The Biochemical Journal* **201**, 189–198.

Besteiro, S., Coombs, G. H. and Mottram, J. C. (2004). A potential role for ICP, a Leishmanial inhibitor of cysteine peptidases, in the interaction between host and parasite. *Molecular Microbiology* **54**, 1224–1236.

Björk, B., Pol, E., Raub-Segall, E., Abrahamson, M., Rowan, A. D. and Mort, J. S. (1994). Differential changes in the association and dissociation rate constants for binding of cystatins to target proteinases occurring on N-terminal truncation of the inhibitors indicate that the interaction mechanism varies with different enzymes. *The Biochemical Journal* **299**, 219–225.

Casados-Vázquez, L. E., Lara-González, S. and Brieba, L. G. (2011). Crystal structure of the cysteine protease inhibitor 2 from *Entamoeba histolytica*: functional convergence of a common protein fold. *Gene* **471**, 45–52.

Cazzulo, J. J. (2002). Proteinases of *Trypanosoma cruzi*: patential targets for the chemotherapy of Changas disease. *Current Topics in Medicinal Chemistry* **2**, 1261–1271.

Chen, X., Xie, S., Bhat, S., Kumar, N., Shapiro, T. A. and Liu, J. O. (2009). Fumagillin and fumarranol interact with *P. falciparum* methionine aminopeptidase 2 and inhibit malaria parasite growth in vitro and in vivo. *Chemical Biology* **16**, 193–202.

Dou, Z. and Carruthers, V. B. (2011). Cathepsin proteases in Toxoplasma gondii. *Advances in Experimental Medicine and Biology* **712**, 49–61.

Ersmark, K., Samuelsson, B. and Hallberg, A. (2006). Plasmepsins as potential targets for new antimalarial therapy. *Medicinal Research Reviews* **26**, 626–666.

Fayer, R., Morgan, U. and Upton, S. J. (2000). Epidemiology of *Cryptosporidium* transmission, detection and identification. *International Journal for Parasitology* **30**, 1305–1322.

Figueiredo da Silva, A. A., Vieira, L .D. C., Krieger, M. A., Goldenberg, S., Zanchin, N. I. T. and Guimaraes, B. G. (2007). Crystal structure of chagasin, the endogenous cysteine-protease inhibitor from *Trypanosoma cruzi*. *Journal of Structural Biology* **157**, 416–423.

Hames, D. B. (1990). One-dimensional polyacrylamide gel electrophoresis. In *Gel Electrophoresis of Proteins* (ed. Hames, D. B. and Rickwood, D.), pp. 1–147. Oxford University Press, New York, USA.

Huang, R., Que, X., Hirata, K., Brinen, L. S., Lee, J. H., Hansell, E., Engel, J., Sajid, M. and Reed, S. (2009). The cathepsin L of *Toxoplasma gondii* (TgCPL) and its endogenous macromolecular inhibitor, toxostatin. *Molecular and Biochemical Parasitology* **164**, 86–94.

Kang, J. M., Sohn, W. M., Ju, J. W., Kim, T. S. and Na, B. K. (2010). Identification and characterization of a serine protease inhibitor of *Clonorchis sinensis*. *Acta Tropica* **116**, 134–140.

Kang, J. M., Lee, K. H., Sohn, W. M. and Na, B. K. (2011*a*). Identification and functional characterization of CsStefin-1, a cysteine protease inhibitor of *Clonorchis sinensis*. *Molecular and Biochemical Parasitology* **177**, 126–134.

Kang, J. M., Ju, H. L., Sohn, W. M. and Na, B. K. (2011*b*). Molecular cloning and characterization of a M17 leucine aminopeptidase of *Cryptosporidium parvum*. *Parasitology* **138**, 682–690.

Knox, D. P. (2007). Proteinase inhibitors and helminth parasite infection. *Parasite Immunology* **29**, 57–71.

Kosek, M., Alcantara, C., Lima, A. A. and Guerrant, R. L. (2001). Cryptosporidiosis: an update. *Lancet Infectious Diseases* **1**, 262–269.

Laskowski, M., Jr. and Kato, I. (1980). Protein inhibitors of proteinases. *Annual Review of Biochemistry* **49**, 593–626.

Lee, J. G., Han, E. T., Park, W. Y. and Yu, J. R. (2009). Ultrastructural localization of *Cryptosporidium parvum* antigen using human patients sera. *Korean Journal of Parasitology* **47**, 171–174.

Ljunggren, A., Redzynia, I., Alvarez-Fernandez, M., Abrahamson, M., Mort, J. S., Krupa, J. C., Jaskolski, M. and Bujacz, G. (2007). Crystal structure of the parasite protease inhibitor chagasin in complex with a host target cysteine protease. *Journal of Molecular Biology* **371**, 137–153.

Monteiro, A. C. S., Abrahamson, M., Lima, A. P. C. A., Vannier-Santos, M. A. and Scharfstein, J. (2001). Identification, characterization and localization of chagasin, a tight-binding cysteine proteases inhibitor in *Trypanosoma cruzi*. *Journal of Cell Science* **114**, 3933–3942.

Na, B. K., Kang, J. M., Cheun, H. I., Cho, S. H., Moon, S. U., Kim, T. S. and Sohn, W. M. (2009). Cryptopain-1, a cysteine protease of *Cryptosporidium parvum*, does not require the pro-domain for folding. *Parasitology* **136**, 149–157.

Pandey, K. C., Singh, N., Arastu-Kapur, S., Bogyo, M. and Rosenthal, P. J. (2006). Falstatin, a cysteine protease inhibitor of *Plasmodium falciparum*, facilitates erythrocyte invasion. *PLoS Pathogens* **2**, e117.

Peterson, C. (1992). Cryptosporidiosis in patients with human immunodeficiency virus. *Clinical Infectious Diseases* **15**, 903–909.

Redzynia, I., Ljunggren, A., Abrahamson, M., Mort, J. S., Krupa, J. C., Jaskolski, M. and Bujacz, G. (2008). Displacement of the occluding loop by the parasite protein, chagasin, results in efficient inhibition of human cathepsin B. *Journal of Biological Chemistry* **283**, 22815–22825.

Redzynia, I., Ljunggren, A., Bujacz, A., Abrahamson, M., Jaskolski, M. and Bujacz, G. (2009). Crystal structure of the parasite inhibitor chagasin in complex with papain allows identification of structural requirements for broad reactivity and specificity determinants for target proteases. *FEBS Journal* **276**, 793–806.

dos Reis, F. C., Smith, B. O., Santos, C. C., Costa, T. F., Scharfstein, J., Coombs, G. H., Mottram, J. C. and Lima, A. P. C. A. (2008). The role of conserved residues of chagasin in the inhibition of cysteine peptidases. *FEBS Letters* **582**, 485–490.

Riekenberg, S., Witjes, B., Šariæ, M., Bruchhaus, I. and Scholze, H. (2005). Identification of EhICP1, a chagasin-like cysteine protease inhibitor of *Entamoeba histolytica*. *FEBS Letters* **579**, 1573–1578.

Rigden, D. J., Mosolov, V. V. and Galperin, M. Y. (2002). Sequence conservation in the chagasin family suggests a common trend in cysteine proteinase binding by unrelated protein inhibitors. *Protein Science* **11**, 1971–1977.

Rosenthal, P. J. (2004). Cysteine proteases of malaria parasites. *Internal Journal for Parasitology* **34**, 1489–1499.

Salmon, D., Aido-Machado, R., Diehl, A., Leidert, M., Schmetzer, O., Lima, A. P. C. A., Scharfstein, J., Oschkinat, H. and Pires, J. R. (2006). Solution structure and backbone dynamics of the *Trypanosoma cruzi* cysteine protease inhibitor chagasin. *Journal of Molecular Biology* **357**, 1511–1521.

Sanderson, S. J., Westrop, J., Scharfstein, J., Mottram, J. C. and Coombs, G. H. (2003). Functional conservation of a natural cysteine peptidase inhibitor in protozoan and bacterial pathogens. *FEBS Letters* **542**, 12–16.

Santos, C. C., Sant'Anna, C., Terres, A., Cunha-e-Silva, N. L., Scharfstein, J. and Lima, A. P. C. A. (2005). Chagasin, the endogenous cysteine-protease inhibitor of *Trypanosoma cruzi*, modulates parasite differentiation and invasion of mammalian cells. *Journal of Cell Science* **118**, 901–915.

Santos, C. C., Scharfstein, J. and Lima, A. P. C. A. (2006). Role of chagasin-like inhibitors as endogenous regulators of cysteine proteases in parasitic protozoa. *Parasitology Research* **99**, 323–324.

Saric, M., Vahrmann, A., Bruchhaus, I., Bakker-Grunwald, T. and Scholze, H. (2006). The second cysteine protease inhibitor, EhICP2, has a different localization in trophozoites of *Entamoeba histolytica* than EhICP1. *Parasitology Research* **100**, 171–174.

Sato, D., Nakada-Tsukui, K., Okada, M. and Nozaki, T. (2006). Two cysteine protease inhibitors, EhICP1 and 2, localized in distinct compartments, negatively regulate secretion in *Entamoeba histolytica*. *FEBS Letters* **580**, 5306–5312.

Smith, B. O., Picken, N. C., Westrop, G. D., Bromek, K., Mottram, J. C. and Coombs, G. H. (2006). The structure of *Leishmania Mexicana Icp* provides evidence for convergent evolution of cysteine peptidase inhibitors. *Journal of Biological Chemistry* **281**, 5821–5828.

Teixeira, C., Gomes, J. R. and Gomes, P. (2011). Falcipains, *Plasmodium falciparum* cysteine proteases as key drug targets against malaria. *Current Medicinal Chemistry* **18**, 1555–1572.

Tzipori, S. and Ward, H. (2002). Cryptosporidosis: biology, pathogenesis and disease. *Microbes and Infection* **4**, 1047–1058.

Wang, S. X., Pandey, K. C., Scharfstein, J., Whisstock, J., Huang, R. K., Jacobelli, J., Fletterick, R. J., Rosenthal, P. J., Abrahamson, M., Brinen, L. S., Rossi, A., Sali, A. and McKerrow, J. H. (2007). The structure of chagasin in complex with a cysteine protease clarifies the binding mode and evolution of an inhibitor family. *Structure* **15**, 535–543.

Wanyiri, J. W., Techasintana, P., O'Connor, R. M., Blackman, M. J., Kim, K. and Ward, H. D. (2009). Role of CpSUB1, a subtilisin-like protease, in *Cryptosporidium parvum* infection in vitro. *Eukaryotic Cell* **8**, 470–477.